Author Manuscript

Author Manuscript

Author Manuscript

Author Manuscript

HHS Public Access

Author manuscript

Mol Pharm. Author manuscript; available in PMC 2016 December 19.

Published in final edited form as:

Mol Pharm. 2015 June 01; 12(6): 1929–1938. doi:10.1021/mp5006917.

Evaluation of ^{68}Ga- and ^{177}Lu-DOTA-PEG$_4$-LLP2A for VLA-4-Targeted PET Imaging and Treatment of Metastatic Melanoma

Wissam Beaino[†,‖], **Jessie R. Nedrow**[†,‖], and **Carolyn J. Anderson**[†,‡,§,*]

[†]Department of Radiology, University of Pittsburgh, Pittsburgh, Pennsylvania 15219, United States

[‡]Department of Pharmacology and Chemical Biology, University of Pittsburgh, Pittsburgh, Pennsylvania 15219, United States

[§]Department of Bioengineering, University of Pittsburgh, Pittsburgh, Pennsylvania 15219, United States

Abstract

Malignant melanoma is a highly aggressive cancer, and the incidence of this disease is increasing worldwide at an alarming rate. Despite advances in the treatment of melanoma, patients with metastatic disease still have a poor prognosis and low survival rate. New strategies, including targeted radiotherapy, would provide options for patients who become resistant to therapies such as BRAF inhibitors. Very late antigen-4 (VLA-4) is expressed on melanoma tumor cells in higher levels in more aggressive and metastatic disease and may provide an ideal target for drug delivery and targeted radiotherapy. In this study, we evaluated ^{177}Lu- and ^{68}Ga-labeled DOTA-PEG$_4$-LLP2A as a VLA-4-targeted radiotherapeutic with a companion PET agent for diagnosis and monitoring metastatic melanoma treatment. DOTA-PEG$_4$-LLP2A was synthesized by solid-phase synthesis. The affinity of ^{177}Lu- and ^{68}Ga-labeled DOTA-PEG$_4$-LLP2A to VLA-4 was determined in B16F10 melanoma cells by saturation binding and competitive binding assays, respectively. Biodistribution of the LLP2A conjugates was determined in C57BL/6 mice bearing B16F10 subcutaneous tumors, while PET/CT imaging was performed in subcutaneous and metastatic models. ^{177}Lu-DOTA-PEG$_4$-LLP2A showed high affinity to VLA-4 with a K_d of 4.1 ± 1.5 nM and demonstrated significant accumulation in the B16F10 melanoma tumor after 4 h (31.5 ± 7.8%ID/g). The tumor/blood ratio of ^{177}Lu-DOTA-PEG$_4$-LLP2A was highest at 24 h (185 ± 26). PET imaging of metastatic melanoma with ^{68}Ga-DOTA-PEG$_4$-LLP2A showed high uptake in sites of metastases and correlated with bioluminescence imaging of the tumors. These data demonstrate that ^{177}Lu-DOTA-PEG$_4$-LLP2A has potential as a targeted therapeutic for treating melanoma as well as other VLA-4-expressing tumors. In addition, ^{68}Ga-DOTA-PEG$_4$-LLP2A is a readily translatable companion PET tracer for imaging of metastatic melanoma.

*Corresponding Author: andersoncj@upmc.edu. Phone: 412-624-6887.

‖**Author Contributions**

These authors contributed equally to this work (W.B. and J.R.N.).

Supporting Information

%ID values of ^{177}Lu- and ^{68}Ga-DOTA-PEG$_4$-LLP2A biodistribution in different organs. The Supporting Information is available free of charge on the ACS Publications website at DOI: 10.1021/mp5006917.

Author Manuscript Author Manuscript Author Manuscript Author Manuscript

Graphical Abstract

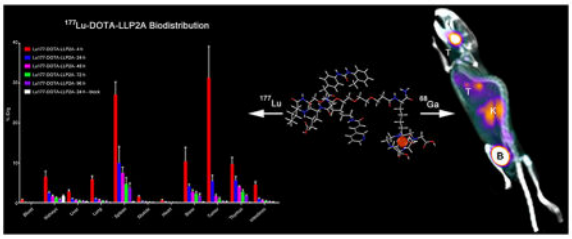

Keywords

LLP2A; VLA-4; lutetium-177; gallium-68; melanoma; PET

INTRODUCTION

The incidence of melanoma is increasing worldwide at a faster rate than other cancers, and metastatic melanoma has an especially poor prognosis.[1] Surgical excision remains the primary treatment for melanoma, with the five-year survival rate being 98% for the localized nonmetastatic disease, 62% for regional metastatic, and 15% for nonregional metastatic disease.[2] A complete lymphadenectomy is recommended for patients with regional lymph node metastases, and for distant metastatic melanoma, surgical removal of the tumor, when possible, is the therapy of choice.[3,4] After several decades of ineffective treatments for metastatic melanoma, there has been a breakthrough of new immunotherapies and targeted therapies over the last 5 years that have changed the course of treating metastatic melanoma.[5]

High-dose interleukin-2 (IL-2) was the first nonspecific immunomodulator approved for treating metastatic melanoma, but this treatment was associated with high clinical toxicity and significant morbidity.[6] A more recent approach in immunotherapy consists in boosting the cell-mediated immunity by blocking the checkpoint molecules like T-lymphocyte associated antigen-4 (CTLA-4) and programmed cell death protein-1 (PD-1), coinhibitory receptors that down-modulate the T-cell response.[7,8] Ipilimumab, a fully human monoclonal antibody, is the first FDA-approved CTLA-4 inhibitor that acts in preventing the down-regulation of T-cell activation and allows a sustainable immune reaction against melanoma tumors. A randomized, phase III clinical study with ipilimumab showed a significant improvement of the overall survival with previously treated stage III/IV melanoma patients.[9] A recent phase II clinical study comparing ipilimumuab, with or without dacarbazine, in chemotherapy-naïve patients showed an increase in the median overall survival for the combined therapy (14.3 months) compared to the monotherapy (11.4 months).[10] Another target for immunotherapy is the PD-1 receptor, which plays a role in T-cell proliferation, survival, and functions.[11] A recent phase I trial with Nivolumab, a fully human IgG4 antibody that blocks PD-1 showed promising results with a median overall survival of 16.8 months and 1 and 2 years overall survival of 62% and 43%.[12] Although there are promising results with immunotherapy, it is associated with severe autoimmune-related adverse effects like diarrhea/colitis, rash, hypothyroidism, and adrenal insufficiency.[13] Clinical

Author Manuscript Author Manuscript Author Manuscript Author Manuscript

investigations of other immunotherapy agents and different drug combinations are still ongoing with encouraging results.[5]

The proto-oncogene BRAF codes for B-Raf, a protein that plays an important role in directing cell growth. A common mutation in melanoma is BRAF-V600E, present in 40–60% of cases.[14] The BRAF-V600E mutation increases the kinase activity and hyperactivation of the mitogen-activated protein kinase (MAPK) pathway, leading to an increase in proliferation, survival, and metastasis.[15] Vemurafenib is a specific and selective potent BRAF V600E inhibitor that showed impressive results in treating metastatic melanoma.[16] In a recent randomized phase III trial, vemurafenib showed a response rate of 48% and 84% in patients with the BRAF-V600E mutation with a detectable decrease in tumor size and a marked increase in the survival rate.[17,18] Dabrafenib is another FDA-approved agent for the treatment of patients with BRAF V600E mutation and unresectable metastatic melanoma.[19] Dabrafenib showed similar overall response rates as vemurafinib but seemed to have an advantage in treating intracranial metastases in patients with advanced melanoma.[20] However, despite these encouraging results, drug resistance develops, and the responses to RAF inhibitors are transient with most patients eventually having recurrence and relapse.[21,22]

In spite of these significant advances in treating metastatic melanoma in the past 5 years, the long-term survival remains less than 10%, and there is an urgent need to develop alternative treatment strategies, especially in patients who develop drug resistance. Lutetium-177 ($T_{1/2}$ = 6.7 days) is a medium energy β-emitter (0.498 MeV [78.6%], 0.176 MeV [12.2%] and 0.385 MeV [9.1%]), which has accompanying γ emissions (0.208 MeV [11%] and 0.113 MeV [6.4%]), making it an ideal radionuclide for treatment of metastatic disease that can be monitored by SPECT imaging. Targeted radiotherapy using ^{177}Lu-DOTA-octreotate has been largely successful for the treatment of neuroendocrine tumors,[23] demonstrating 50% tumor regression for 28% of patients, 25–50% tumor regression for 19% of patients, and stabilization of the disease was achieved for 35% of patients.[24] In addition, targeted radiotherapy with ^{177}Lu-DOTA-octreotate is relatively safe with less toxicity than standard chemotherapy and is generally well tolerated by patients.[25]

Very late antigen-4 (VLA-4; also called integrin $\alpha_4\beta_1$) is a trans-membrane noncovalent heterodimer expressed in melanoma that plays a role in tumor growth, angiogenesis and metastasis by promoting adhesion and migration of tumor cells.[26–28] A high-affinity peptidomimetic ligand (LLP2A) targeted to VLA-4 was identified from a one-bead-one-compound library.[29] In a previous study, we demonstrated that the modified LLP2A conjugates, CB-TE1A1P-PEG$_4$-LLP2A and NODAGA-PEG$_4$-LLP2A, labeled with ^{64}Cu and/or ^{68}Ga, bound with high affinity to VLA-4 in B16F10 melanoma cells (in vitro) and accumulated in VLA-4-positive mouse melanoma tumors (in vivo) with high tumor/muscle and tumor/blood ratios.[30]

In this study, we evaluated the LLP2A conjugate, DOTA-PEG$_4$-LLP2A labeled with ^{177}Lu, to determine its potential as a theranostic agent for metastatic melanoma. The binding affinity and the in vivo performance of the conjugate were investigated using the VLA-4-positive B16F10 mouse melanoma cell line. ^{177}Lu has the added advantage that the uptake

Author Manuscript Author Manuscript Author Manuscript Author Manuscript

can be monitored by SPECT imaging, although the relatively low abundance of emitted gamma rays is not ideal. PET imaging provides higher sensitivity leading to improved image quality compared to SPECT imaging. Therefore, we opted to explore a companion PET agent utilizing the DOTA-PEG_4-LLP2A targeting scaffold labeled with ^{68}Ga for the diagnosis of metastatic melanoma and monitoring of treatment response.

MATERIALS AND METHODS

Reagents

All chemicals were purchased from Sigma-Aldrich Chemical Co. (St. Louis, MO), unless otherwise specified. Aqueous solutions were prepared using ultrapure water (resistivity, 18.2 MΩ·cm). Rink amide 4-methylbenzhydrylamine resin (loading, 0.77 mmol/g), and all Fmoc-protected amino acid were purchased from Chem-Impex International, Inc. (Wood Dale, IL). DOTA was purchased from CheMatec (Dijon, France). Fmoc-PEG_4 carboxylic acid was purchased from ChemPep Inc. (Wellington, FL). $^{177}LuCl_3$ was purchased from the University of Missouri Research Reactor Center (Columbia, MO). Analytical and semipreparative reversed-phase high-performance liquid chromatography (HPLC) were performed on a Waters 1525 Binary HPLC pump (Milford, MA) with a Waters 2489 UV–vis detector and a model 106 Bioscan radioactivity detector (Bioscan Inc., Washington, DC). Nonradioactive HPLC samples were analyzed on an analytical Jupiter C18 column and purified on a semipreparative Jupiter C18 column (Phenomenex, Torrance, CA). Radiochemistry reaction progress and purity were monitored on a Jupiter C18 column (Phenomenex, Torrance, CA). Radioactive samples were counted using either an automated Packard Cobra II gamma counter (Packard, Ramsey, MN) or a PerkinElmer 2470 WIZARD^2 Automatic Gamma Counter (Waltham, MA). PET/CT data were acquired using an Inveon Preclinical Imaging Station (Siemens Medical Solutions).

Peptide Synthesis of DOTA-PEG_4-LLP2A

LLP2A (0.1 mmol) was synthesized using Fmoc/tBu strategy on a rink amide resin (loading, 0.77 mmol/g). First, Fmoc-Lys(Dde)–OH was attached to the resin followed by the PEG linker (Fmoc-PEG_4-COOH) and then the LLP2A was assembled to the N-terminal of the linker. After synthesis, the peptide-resin (50 mg) was resuspended in DMF, the Dde protecting group was cleaved with 2% hydrazine in DMF (3 × 15 min), and the beads were washed with DMF (6 × 1 min). DOTA solubilized in DMF was added to the beads and allowed to react overnight under agitation. Cleavage of the peptide from the resin and removal of the protecting groups was achieved using a mixture of TFA (95%), triisopropylsilane (2.5%), and water (2.5%) for 3 h at room temperature. The compound was characterized by analytical HPLC on a Jupiter C18 column (300 Å pore size, 5 μm particle size, 150 × 4.6 mm) and identified by electrospray mass spectroscopy (mass calculated MW 1571.8 Da, measured MW 1571.3 Da). The purity was greater than 98%.

Radiolabeling of DOTA-PEG_4-LLP2A with Gallium-68 (^{68}Ga) and Lutetium-177 (^{177}Lu)

^{68}Ga was eluted from a $^{68}Ge/^{68}Ga$ generator using 0.1 N HCl and purified using a cation exchange column (Phenomenex, x-c catridges, Torrance, CA). The ^{68}Ga was eluted with 97.5% acetone, 2.25% H_2O, and 0.25% HCl (30%, ultrapure) solution (800 μL).

Author Manuscript Author Manuscript Author Manuscript Author Manuscript

Radiolabeling was conducted at pH 4 in 0.5 M ammonium acetate buffer. DOTA-PEG_4-LLP2A (1 μg) in 100 μL of acetate buffer (pH 4) was mixed with $^{68}GaCl_3$ (37 MBq) in the reaction vessel. The mixture was heated at 70 °C for 30 min for labeling and to evaporate the acetone. Radiolabeling with ^{177}Lu was conducted at pH 5 in 0.1 M ammonium acetate buffer. DOTA-PEG_4-LLP2A (2–7 μg) in 100–300 μL of 0.1 M ammonium acetate buffer (pH 5) and 1–7 μL of 56 mM gentisic acid was mixed with $^{177}LuCl_3$ (54–200 MBq) in the reaction vessel and heated at 70 °C for 30 min. After incubation, the radiochemical purity of the ^{68}Ga- and ^{177}Lu-labeled DOTA-PEG_4-LLP2A was monitored by radio-HPLC with a rocket C18 column (7 × 53 mm, 3 μm; Alltima). The radiolabeled peptides were analyzed using a stepwise gradient from 3% to 97% B over 11 min. Solvent A was H_2O/0.1% TFA and solvent B was CH_3CN/0.1% TFA. The radiochemical purity of both agents was greater than 98%.

Binding Assay

Cell experiments were performed to determine the binding affinity of ^{177}Lu-DOTA-PEG_4-LLP2A in VLA-4-positive B16F10 mouse melanoma cells. Cells were seeded in 24-well plates (100 000 cells per well) 24 h prior to the experiment. Before the experiment, cells were washed twice with HBSS (1 mL), and 0.5 mL binding media (HBSS with 0.1% BSA and 1 mM Mn^{2+}) was added to each well. Then 15 μg of LLP2A-PEG_4 was added to half of the wells as a cold block to determine nonspecific binding, followed by ^{177}Lu-DOTA-PEG_4-LLP2A in increasing concentrations (0.2–40 nM). The samples were incubated for 2 h on ice. After incubation, the radioactive media was removed. Cells were rinsed twice with ice cold binding buffer (1 mL) and dissolved in 0.5% SDS solution. The radioactivity in each fraction was measured in a well counter (Packard Cobra II gamma counter). The protein content of each cell lysate sample was determined (BCA Protein Assay Kit, Pierce). The measured radioactivity associated with the cells was normalized to the amount of cell protein present (cpm/mg protein). The K_d and B_{max} were calculated using PRISM 5 (GraphPad; La Jolla, CA).

The competitive binding assay of Ga-DOTA-PEG_4-LLP2A was performed by competition with ^{64}Cu-NODAGA-PEG_4-LLP2A in VLA-4-positive B16F10 mouse melanoma cells. ^{nat}Ga-DOTA-PEG_4-LLP2A was prepared with an excess of cold gallium (100-fold) under the same conditions as the ^{68}Ga-labeled peptide (pH 4, 70 °C, 20 min). Cells were seeded in 24-well plates (100 000 cells per well) 24 h prior to the experiment. Before the experiment, cells were washed twice with 1 mL HBSS. Then ^{64}Cu-NODAGA-PEG_4-LLP2A (1.1 nM) was added to increasing concentrations of Ga-DOTA-PEG_4-LLP2A (0.005, 0.015, 0.05, 0.15, 0.5, 1.5, 5, 50, 500, 5000, 50000 nM) in 0.5 mL of binding media (HBSS with 0.1% BSA and 1 mM Mn^{2+}) in quadruplicate. The samples were incubated for 3 h on ice. After incubation, the radioactive media was removed. Cells were rinsed with ice-cold binding buffer (1 mL) twice and dissolved in 0.5% SDS. The radioactivity in each fraction was measured in a gamma counter (Packard Cobra II gamma counter). The protein content of each cell lysate sample was determined (BCA Protein Assay Kit, Pierce). The measured radioactivity associated with the cells was normalized to the amount of cell protein present (cpm/mg protein). The K_i and IC_{50} were calculated using PRISM 5.

Author Manuscript Author Manuscript Author Manuscript Author Manuscript

Internalization Assay

Internalization studies were performed as previously described.[31] Briefly, aliquots of B16F10 cells (2×10^5 cells) were placed in 12-well plates and incubated overnight. The wells were prepared as previously described,[31] and ^{177}Lu-DOTA-PEG$_4$-LLP2A (12 ng/10 μL) was added to blocked and unblocked wells ($n = 3$). Blocked wells were pretreated with 10 μg of LLP2A-PEG$_4$. The cells were allowed to incubate for 15 min, 30 min, 2 h, and 4 h at 37 °C. Following incubation, the media was collected in separate fractions; the surface-bound and the lysed cells were counted on a Packard Cobra II automated γ-counter. The total protein concentration in the cell lysate was determined using the BCA Protein Assay. Internalized agent was expressed as fmol/mg of protein.

Animal Studies

Four to six week old male C57BL/6 mice from Jackson laboratories (Bar Harbor, Maine) and 6 to 8 week old female albino C57BL/6 mice from Charles River (Malvern, Pennsylvania) were used in this study. All animal studies were performed under the Guide for the Care and Use of Laboratory Animals under the auspices of Division of Laboratory Animal Resources (DLAR) under a protocol approved by the University of Pittsburgh Institutional Animal Care and Use Committee (IACUC). For xenograft B16F10 tumors, mice (6 to 8 weeks old) were injected subcutaneously in the right shoulder with 10^6 cells in PBS. For the melanoma metastatic model, 6 to 8 weeks old albino C57BL/6 mice were injected with 2×10^5 cells in the left ventricle.

Biodistribution Experiments

B16F10 tumor bearing C57BL/6 mice were injected intravenously with ^{68}Ga-DOTA-PEG$_4$-LLP2A (5.55 MBq, 277 ng) ($n = 4$ per group) or ^{177}Lu-DOTA-PEG$_4$-LLP2A (3.6 MBq, 90 ng) ($n = 5$ per group). The tumor-bearing mice were sacrificed at 1 h postinjection for the ^{68}Ga biodistribution and at 4, 24, 48, 72, and 96 h for the ^{177}Lu biodistribution. The blood, heart, intestines, lungs, liver, spleen, kidneys, muscle, bone, thymus and tumor were harvested, weighed, and counted in a γ-counter. An additional group of mice was injected with ^{68}Ga or ^{177}Lu labeled radiopharmaceuticals premixed with 100 μg of LLP2A-PEG$_4$ to serve as a blocking agent and sacrificed at 1 or 24 h. The percent injected dose per gram of tissue (% ID/g) was determined by decay correction for each sample normalized to a standard of known weight, which was representative of the injected dose.

PET/CT Imaging and Analysis

C57BL/6J xenograft tumor-bearing ($n = 6$) or intracardiac injected mice ($n = 3$) were injected intravenously (lateral tail vein) with ^{68}Ga-DOTA-PEG$_4$-LLP2A (7.4 MBq, 370 ng). Half of the xenograft tumor-bearing mice received a dose that was premixed with LLP2A-PEG$_4$ (50 μg) for blocking. Imaging was done at 1 h postinjection, mice were anaesthetized with 2% isoflurane, and small animal PET/CT was performed. Static images were collected for 10 min using a small animal Inveon PET/CT scanner (Siemens Medical Solution, Knoxville, TN). Tangential and radial full width at half-maximum are 1.5 mm at the center of field of view (FOV) and 1.8 mm at the edge of FOV. PET and CT images were coregistered with Inveon Research Workstation (IRW) software (Siemens Medical Solutions,

Author Manuscript Author Manuscript Author Manuscript Author Manuscript

Knoxville, TN). PET images were reconstructed with the Ordered-Subsets Expectation Maximization 3D/maximum aposteriori probability (OSEM-3D) algorithm, and the analysis of images was done using IRW software. Regions of interest (ROI) were drawn on the basis of the CT, and the associated PET activities were calculated. Standard uptake values (SUVs) were calculated based on the following formula: SUV = ([Bq/mL] × [animal weight (g)]/[injected dose (Bq)]).

Stability of ^{177}Lu- DOTA-PEG$_4$-LLP2A

To determine the bench stability of ^{177}Lu- DOTA-PEG$_4$-LLP2A in labeling buffer, the conjugate was analyzed at 30 min, 1 and 24 h postlabeling by radio-HPLC on a rocket C18 column (7 × 53 mm, 3 μm; Alltima).

Statistical Analysis

All data are presented as mean ± standard deviation. Groups were compared using PRISM 5 two tailed student *t*-test or two-way Anova. Values of $p < 0.05$ were considered statistically significant.

RESULTS

Radiochemistry and Stability

The ^{177}Lu-DOTA-PEG$_4$-LLP2A conjugate (Figure 1A) was radiolabeled in 30 min at 70 °C in ammonium acetate buffer with gentisic acid at a specific activity of 27–29 MBq/μg with >98% radiochemical purity. The ^{68}Ga-DOTA-PEG$_4$-LLP2A conjugate was radiolabeled in 30 min at 70 °C in ammonium acetate buffer at a specific activity of 37 MBq/μg with >98% radiochemical purity. ^{177}Lu is a beta emitter and can induce radiolysis of the conjugate. To ensure stability of the ^{177}Lu-labeled LLP2A conjugate, gentisic acid was added as a radical scavenger. We investigated its bench stability, and we found that the ^{177}Lu conjugate was stable for 24 h at room temperature, with no radiolysis products detected by radio-HPLC (Figure 2).

Cell Binding Assay

Saturation binding assay shows that ^{177}Lu-DOTA-PEG$_4$-LLP2A binds with high affinity to the VLA-4 with a K_d of 4.1 ± 1.5 nM and B_{max} of 631 ± 70.2 fmol/mg (Figure 1B). Gallium-68 has a short half-life (68 min), and it is not suitable for the saturation-binding-assay conditions. Therefore, a competitive binding assay was performed to evaluate the half-maximal inhibitory concentration (IC_{50}) and the inhibitor constant (K_i) of cold ^{nat}Ga-DOTA-PEG$_4$-LLP2A. The competitive binding assay was performed by competing the cold ^{nat}Ga-DOTA-PEG$_4$-LLP2A with ^{64}Cu-NODAGA-PEG$_4$-LLP2A in B16F10 cells at 4 °C (Figure 1C). ^{nat}Ga-DOTA-PEG$_4$-LLP2A binds with higher affinity to VLA-4 compared to ^{177}Lu-DOTA-PEG$_4$-LLP2A with a K_i of 1.56 nM (95% confidence intervals 1.3–1.8) and an IC_{50} of 9.37 nM (95% confidence intervals 7.8–11.2); however, Ga-DOTA-PEG$_4$-LLP2A has around 15-fold lower affinity compared to previously reported Ga-NODAGA-PEG$_4$-LLP2A.[30]

Author Manuscript Author Manuscript Author Manuscript Author Manuscript

Internalization of ^{177}Lu-DOTA-PEG$_4$-LLP2A

Internalization of ^{177}Lu-DOTA-PEG$_4$-LLP2A was evaluated in B16F10 melanoma cells (Figure 3). The compound internalized rapidly (<15 min post addition), reaching maximum uptake at 30 min (341 ± 110 fmol/mg), and then plateaued at 2 and 4 h (343 ± 53 fmol/mg and 303 ± 41 fmol/mg, respectively).

Biodistribution Studies

Biodistribution of ^{177}Lu-DOTA-PEG$_4$-LLP2A—The biodistribution of ^{177}Lu-DOTA-PEG$_4$-LLP2A in B16F10 tumor-bearing mice was determined at 4, 24, 48, 72, and 96 h postprobe injection (Figure 4). At 4 h postinjection, ^{177}Lu-DOTA-PEG$_4$-LLP2A accumulated in the tumor (31.3 ± 7.8% ID/g) as well as in VLA-4 rich organs such as spleen (27.1 ± 3.1% ID/g), bone (likely bone marrow; 10.1 ± 3.5% ID/g), and thymus (9.7 ± 1.7% ID/g). The probe cleared primarily through the kidneys (6.5 ± 1.5% ID/g) with lower liver uptake (2.8 ± 0.4% ID/g). A relatively high uptake was observed in the lungs (5.9 ± 0.8% ID/g) with minimal uptake in the muscle, heart, and blood. At 24 h, the probe started to clear from targeted and nontargeted organs, and we observed a significant decrease in uptake: tumor (5.4 ± 1.5% ID/g), spleen (10.1 ± 4.1% ID/g), bone (4.1 ± 0.4% ID/g), thymus (5.6 ± 0.9% ID/g), and all the nontargeted organs. At 48, 72, and 96 h, the ^{177}Lu-DOTA-PEG$_4$-LLP2A continued to clear from tumor (1.7 ± 0.4; 0.9 ± 0.4 and 0.4 ± 0.07% ID/g, respectively), spleen (7.4 ± 1.4; 4.7 ± 1.5 and 3.7 ± 1.1% ID/g, respectively), bone (2.7 ± 0.6; 2.2 ± 0.5 and 1.6 ± 0.6% ID/g, respectively), and thymus (4.1 ± 0.2; 2.7 ± 0.5 and 1.7 ± 0.2% ID/g, respectively). ^{177}Lu-DOTA-PEG$_4$-LLP2A demonstrated a high tumor/blood ratio at 4 h (36 ± 10), reaching a peak at 24 h (186 ± 26), followed by a steady decrease at 48, 72, and 96 h (61 ± 13; 35 ± 37; 25 ± 16, respectively) (Figure 5A). The tumor/muscle ratio of ^{177}Lu-DOTA-PEG$_4$-LLP2A was highest at 4 h (21 ± 7) and then decreased at 24, 48, 72, and 96 h (18 ± 3; 9 ± 1; 6 ± 3; 3 ± 0.4, respectively) (Figure 5B). In the presence of blocking agent (LLP2A-PEG$_4$, 1100-fold), ^{177}Lu-DOTA-PEG$_4$-LLP2A demonstrated significant reduction of uptake, with ≤0.2% ID/g found in the tumor and VLA-4-positive tissues. These blocking effects indicate selective binding of VLA-4 for ^{177}Lu-DOTA-PEG$_4$-LLP2A.

Biodistribution of ^{68}Ga-DOTA-PEG$_4$-LLP2A—^{68}Ga-DOTA-PEG$_4$-LLP2A had high accumulation in the B16F10 tumor at 1 h (9.1 ± 0.9% ID/g) and was cleared primarily through the kidneys (3.7 ± 0.9% ID/g); the liver uptake was 1.9 ± 0.4% ID/g (Figure 6A). The ^{68}Ga-agent had tumor/muscle and tumor/blood ratios of 9.7 ± 1.5 and 5.8 ± 1.5, respectively (Figure 6B). Uptake was also observed in VLA-4-positive organs such as the spleen, bone marrow, and thymus (5.4 ± 1.7, 3.2 ± 0.7 and 4.6 ± 0.5% ID/g, respectively). A blocking study with 360-fold excess of LLP2A-PEG$_4$ at 1 h demonstrated reduction of uptake of ^{68}Ga-DOTA-PEG$_4$-LLP2A, indicating the targeting specificity for VLA-4.

PET Imaging of ^{68}Ga-DOTA-PEG$_4$-LLP2A in B16F10 Subcutaneous Tumor-Bearing Mice and Metastatic B16F10 Melanoma

PET/CT images of ^{68}Ga-DOTA-PEG$_4$-LLP2A demonstrated high contrast in the tumor compared to background and the VLA-4-positive organs, such as the spleen, thymus, and

Author Manuscript Author Manuscript Author Manuscript Author Manuscript

bone marrow (Figure 7). ^{68}Ga-DOTA-PEG$_4$-LLP2A cleared through the kidneys with significant accumulation in the bladder, indicating that rapid renal clearance. Reduction of the tumor to background levels was observed when a blocking agent was administered prior to the probe further supporting the probes selectivity for VLA-4. In addition, ^{68}Ga-DOTA-PEG$_4$-LLP2A visualized small metastases in the lungs and bones (metastases size 1–2 mm) at 1 h (Figure 8C,D,E) in high contrast to the background and other VLA-positive organs. The uptake of the probe correlated with the bioluminescent images of tumor metastases (Figure 8A,E). In addition, the uptake in the lungs correlated with metastases, as identified by CT (Figure 8D).

DISCUSSION

Malignant melanoma is a very aggressive type of cancer, and there has been an alarming increase in incidence worldwide. Significant progress has been made for treating melanoma, particularly with targeted therapy,[17,18] but despite these advances, patients with metastatic disease still have poor prognosis and low survival rate. New strategies are needed for more effective treatment and better tumor targeting, especially when surgical intervention is not feasible. VLA-4 is known to be expressed on melanoma tumor cells with increased expression in more aggressive and metastatic disease states. Thus, VLA-4 may provide an ideal target for drug delivery and targeted radiotherapy.

We previously demonstrated that ^{64}Cu and/or ^{68}Ga labeled NODAGA-PEG$_4$-LLP2A and CB-TE1A1P-PEG$_4$-LLP2A bound with high affinity to VLA-4 showing high accumulation in subcutaneous and metastatic VLA-4-positive tumors.[30] These factors prompted us to evaluate a LLP2A conjugate as a potential radiotherapeutic for metastatic melanoma. We selected the DOTA chelator due to its ability to stably complex ^{177}Lu for cancer therapy and ^{68}Ga for PET imaging.

The affinity of the ^{68}Ga-labeled conjugate was 3-fold higher than the ^{177}Lu-labeled conjugate; however, the affinity of ^{68}Ga-DOTA-PEG$_4$-LLP2A was 15-fold lower than the previously reported ^{68}Ga-NODAGA-PEG$_4$-LLP2A, presumably due to changes in overall structure and lipophilicity of the agent.[32,33] Despite the decreased affinity of ^{68}Ga-DOTA-PEG$_4$-LLP2A for VLA-4 compared to ^{68}Ga-NODAGA-PEG$_4$-LLP2A, the biodistribution was improved with less kidney retention (3.7 ± 0.9% ID/g for DOTA vs 7.0 ± 3.7% ID/g for NODAGA) and less liver uptake (1.9 ± 0.4% ID/g DOTA vs 3.6 ± 1.3% ID/g NODAGA) for the DOTA conjugate while the tumor uptake remained comparable.

The in vivo biodistribution of ^{68}Ga-DOTA-PEG$_4$-LLP2A was encouraging and supported the investigation of ^{177}Lu-DOTA-PEG$_4$-LLP2A as a potential agent for targeted radiotherapy. ^{177}Lu-DOTA-PEG$_4$-LLP2A exhibited very high tumor uptake at 4 h (31.3 ± 7.8%ID/g) that significantly decreased after 24 h to 5.4 ± 1.5%ID/g and continued to clear out of the tumor over the 96 h window. It is important to note that the uptake of ^{177}Lu-labeled conjugate in the tumor decreased at a faster rate than the VLA-4-positive organs, most likely due in part to the fast growth rate of the B16F10 tumors, which increased 50–100% in size over a 24 h period and increased in size 4–6-fold from day 1 to day 4 postinjection of the ^{177}Lu-DOTA-PEG$_4$-LLP2A. This rapid growth rate of the B1610 tumor

Author Manuscript Author Manuscript Author Manuscript Author Manuscript

model impacts the calculation of %ID/g of the ^{177}Lu-DOTA-PEG$_4$-LLP2A due to the dilution effect of the dose as a consequence of the fast tumor growth. Another possible explanation for the decreasing tumor uptake over time compared to the other VLA-4-positive organs is tumor metabolism of the LLP2A conjugate leading to washout of the compound from the tumor. We believe this is unlikely, however, because LLP2A is highly stable in serum and resistant to proteases,[29,30] and the ^{177}Lu-DOTA chelate is highly stable.[34] Additionally, the near-complete blood clearance of ^{177}Lu-DOTA-PEG$_4$-LLP2A to 0.01%ID/g suggests high in vivo stability.

The positive initial in vivo results of ^{177}Lu-DOTA-PEG$_4$-LLP2A are encouraging for translation to targeted radiotherapy in humans. One of the critical limitations of targeted radiotherapy is the destruction or toxicity induced by the radiation in excretion organs and receptor-positive normal tissues, which can limit the radiotherapeutic dose that can be safely administered. ^{177}Lu-DOTA-PEG$_4$-LLP2A demonstrated low liver uptake (1.0 ± 0.1%ID/g at 24 h) and rapid kidney clearance (2.4 ± 0.3% ID/g at 24 h), which is advantageous for radiotherapy. However, the high uptake of ^{177}Lu-DOTA-PEG$_4$-LLP2A in receptor-positive organs like spleen, thymus, and bone marrow, due to the expression of the VLA-4 on the immune cells, is of potential concern. Kulkarni et al. demonstrated that a high radiotherapeutic dose to the spleen of ^{177}Lu-DOTATATE/TOC in patients showed no significant hematological toxicity, and there was no correlation between the incidence or grade of toxicity and the dose to the spleen.[35] The thymus uptake of ^{177}Lu-DOTA-PEG$_4$-LLP2A was moderate but rapidly cleared over the 96 h window and is not expected to be a dose-limiting organ. The high accumulation of ^{177}Lu-DOTA-PEG$_4$-LLP2A in the bone marrow may be a limiting factor for the maximum tolerated dose. Bone marrow toxicity is an issue with antibodies due to their long circulation times, allowing the bone marrow to be exposed over a long window; however, ^{177}Lu-DOTA-PEG$_4$-LLP2A demonstrated rapid clearance from the blood. The combination of rapid blood clearance and clearance of the probe from the bone over the 96 h window may reduce the exposure of the bone marrow. Additional studies, particularly dosimetry estimates to VLA-4-positive organs, are needed prior to evaluating this agent as a radiotherapeutic agent in tumor-bearing mice.

The expression level of VLA-4 on primary melanoma tumors correlates with the development of metastases.[36] Melanoma tumors having high VLA-4 expression are associated with a greater risk of metastasis and tumor progression.[37,38] Thus, PET imaging of VLA-4 with ^{68}Ga-DOTA-PEG$_4$-LLP2A may identify patients who will benefit from targeted therapy with ^{177}Lu-DOTA-PEG$_4$-LLP2A and also in monitoring the treatment response. ^{68}Ga-DOTA-PEG$_4$-LLP2A demonstrated accumulation in B16F10 melanoma tumor (9.1 ± 0.9% ID/g) with reasonably high tumor/muscle (9.7 ± 1.5) and tumor/blood (5.8 ± 1.5) ratios. Even though ^{68}Ga-DOTA-PEG$_4$-LLP2A demonstrated a lower affinity for VLA-4 compared to the previously reported ^{68}Ga-NODAGA-PEG$_4$-LLP2A, it demonstrated a more desirable in vivo performance with lower liver, kidneys, and spleen uptake. Although this was somewhat surprising, it is often difficult to predict in vivo behavior based on in vitro binding affinity, or to predict which chelators will give the most optimal biodistributions.[30,39,40] ^{68}Ga-DOTA-PEG$_4$-LLP2A imaged B16F10 subcutaneous melanoma tumors, but more importantly, it was able to detect small metastases in lungs and bones with high contrast and sensitivity (tumor size of 1–2 mm). The facile labeling of ^{68}Ga and it

Author Manuscript Author Manuscript Author Manuscript Author Manuscript

being available on-site at a relatively low cost from a $^{68}Ge/^{68}Ga$ generator makes ^{68}Ga-DOTA-PEG_4-LLP2A a tracer that can be readily translated into human studies.

Melanocortin 1 receptor (MC1-R) is another melanoma biomarker that has been widely explored for specific imaging and targeted radiotherapy in metastatic melanoma.[41] Despite the high specificity of the MC1-R for melanoma, extremely high specific activity labeled compounds are required due to the low level of expression of MC1-R on melanoma cells, which requires HPLC-purification of the final product from any unlabeled precursors.[42,43] In addition, endogenous MC1-R ligands can compete with the radioligand and can reduce the cell surface receptor due to internalization.[44] The higher expression of VLA-4 on melanoma tumors, particularly in tumors that are metastatic, may provide an alternative to MC1-R as a molecular target for radiotherapy in patients with metastatic melanoma.

CONCLUSION

Data presented here demonstrate the potential of ^{177}Lu- and ^{68}Ga-labeled DOTA-PEG_4-LLP2A as a VLA-4-targeted radiotherapeutic with a companion PET agent for diagnosis, treatment, and monitoring of metastatic melanoma. The high uptake of ^{177}Lu-DOTA-PEG_4-LLP2A in melanoma tumors with kidney clearance suggests that it might have other applications for therapy in other VLA-4-positive cancers such as multiple myeloma and lymphoma. The combination of ^{177}Lu-DOTA-PEG_4-LLP2A with other therapies, including BRAF inhibitors, immunotherapy, chemotherapy, or adjuvant therapy, may improve/increase the overall survival in patients with metastatic melanoma. Finally, ^{177}Lu-DOTA-PEG_4-LLP2A may provide another treatment option to patients with metastatic melanoma who have failed other first line treatments.

Supplementary Material

Refer to Web version on PubMed Central for supplementary material.

Acknowledgments

The authors are grateful to Kathryn Day and Joseph Latoche for maintaining the preclinical PET/CT imaging facility.

References

1. Lens MB, Dawes M. Global perspectives of contemporary epidemiological trends of cutaneous malignant melanoma. Br J Dermatol. 2004; 150:179–185. [PubMed: 14996086]
2. Khan MK, Khan N, Almasan A, Macklis R. Future of radiation therapy for malignant melanoma in an era of newer, more effective biological agents. OncoTargets Ther. 2011; 4:137–148.
3. Garbe C, Peris K, Hauschild A, Saiag P, Middleton M, Spatz A, Grob JJ, Malvehy J, Newton-Bishop J, Stratigos A, Pehamberger H, Eggermont AM. Diagnosis and treatment of melanoma. European consensus-based interdisciplinary guideline–Update 2012. Eur J Cancer. 2012; 48:2375–2390. [PubMed: 22981501]
4. Coit DG, Andtbacka R, Bichakjian CK, Dilawari RA, Dimaio D, Guild V, Halpern AC, Hodi FS, Kashani-Sabet M, Lange JR, Lind A, Martin L, Martini MC, Pruitt SK, Ross MI, Sener SF, Swetter SM, Tanabe KK, Thompson JA, Trisal V, Urist MM, Weber J, Wong MK. Melanoma. J Natl Compr Cancer Network. 2009; 7:250–275.

Author Manuscript Author Manuscript Author Manuscript Author Manuscript

5. Shah DJ, Dronca RS. Latest advances in chemotherapeutic, targeted, and immune approaches in the treatment of metastatic melanoma. Mayo Clin Proc. 2014; 89:504–519. [PubMed: 24684873]
6. Schwartz RN, Stover L, Dutcher J. Managing toxicities of high-dose interleukin-2. Oncology (Williston Park). 2002; 16:11–20.
7. Dunn GP, Koebel CM, Schreiber RD. Interferons, immunity and cancer immunoediting. Nat Rev Immunol. 2006; 6:836–848. [PubMed: 17063185]
8. Disis ML. Immune regulation of cancer. J Clin Oncol. 2010; 28:4531–4538. [PubMed: 20516428]
9. Hodi FS, O'Day SJ, McDermott DF, Weber RW, Sosman JA, Haanen JB, Gonzalez R, Robert C, Schadendorf D, Hassel JC, Akerley W, van den Eertwegh AJ, Lutzky J, Lorigan P, Vaubel JM, Linette GP, Hogg D, Ottensmeier CH, Lebbe C, Peschel C, Quirt I, Clark JI, Wolchok JD, Weber JS, Tian J, Yellin MJ, Nichol GM, Hoos A, Urba WJ. Improved survival with ipilimumab in patients with metastatic melanoma. N Engl J Med. 2010; 363:711–723. [PubMed: 20525992]
10. Hersh EM, O'Day SJ, Powderly J, Khan KD, Pavlick AC, Cranmer LD, Samlowski WE, Nichol GM, Yellin MJ, Weber JS. A phase II multicenter study of ipilimumab with or without dacarbazine in chemotherapy-naive patients with advanced melanoma. Invest New Drugs. 2011; 29:489–498. [PubMed: 20082117]
11. Tseng SY, Otsuji M, Gorski K, Huang X, Slansky JE, Pai SI, Shalabi A, Shin T, Pardoll DM, Tsuchiya H. B7-DC, a new dendritic cell molecule with potent costimulatory properties for T cells. J Exp Med. 2001; 193:839–846. [PubMed: 11283156]
12. Sznol M, Kluger HM, Hodi FS, McDermott DF, Carvajal RD, Lawrence DP, Topalian SL, Atkins MB, Powderly JD, Sharfman WH, Puzanov I, Smith DC, Wigginton JM, Kollia G, Gupta AK, Sosman JA. Survival and long-term follow-up of safety and response in patients (pts) with advanced melanoma (MEL) in a phase I trial of nivolumab (anti-PD-1; BMS-936558; ONO-4538). J Clin Oncol. 2013; 31 Suppl Abstract CRA9006.
13. O'Day SJ, Maio M, Chiarion-Sileni V, Gajewski TF, Pehamberger H, Bondarenko IN, Queirolo P, Lundgren L, Mikhailov S, Roman L, Verschraegen C, Humphrey R, Ibrahim R, de Pril V, Hoos A, Wolchok JD. Efficacy and safety of ipilimumab monotherapy in patients with pretreated advanced melanoma: a multicenter single-arm phase II study. Ann Oncol. 2010; 21:1712–1717. [PubMed: 20147741]
14. Flaherty KT. Chemotherapy and targeted therapy combinations in advanced melanoma. Clin Cancer Res. 2006; 12:2366s–2370s. [PubMed: 16609060]
15. Satyamoorthy K, Li G, Gerrero MR, Brose MS, Volpe P, Weber BL, Van Belle P, Elder DE, Herlyn M. Constitutive mitogen-activated protein kinase activation in melanoma is mediated by both BRAF mutations and autocrine growth factor stimulation. Cancer Res. 2003; 63:756–759. [PubMed: 12591721]
16. Bollag G, Hirth P, Tsai J, Zhang J, Ibrahim PN, Cho H, Spevak W, Zhang C, Zhang Y, Habets G, Burton EA, Wong B, Tsang G, West BL, Powell B, Shellooe R, Marimuthu A, Nguyen H, Zhang KY, Artis DR, Schlessinger J, Su F, Higgins B, Iyer R, D'Andrea K, Koehler A, Stumm M, Lin PS, Lee RJ, Grippo J, Puzanov I, Kim KB, Ribas A, McArthur GA, Sosman JA, Chapman PB, Flaherty KT, Xu X, Nathanson KL, Nolop K. Clinical efficacy of a RAF inhibitor needs broad target blockade in BRAF-mutant melanoma. Nature. 2010; 467:596–599. [PubMed: 20823850]
17. Young K, Minchom A, Larkin J. BRIM-1, –2 and –3 trials: improved survival with vemurafenib in metastatic melanoma patients with a BRAF(V600E) mutation. Future Oncol. 2012; 8:499–507. [PubMed: 22646765]
18. Chapman PB, Hauschild A, Robert C, Haanen JB, Ascierto P, Larkin J, Dummer R, Garbe C, Testori A, Maio M, Hogg D, Lorigan P, Lebbe C, Jouary T, Schadendorf D, Ribas A, O'Day SJ, Sosman JA, Kirkwood JM, Eggermont AM, Dreno B, Nolop K, Li J, Nelson B, Hou J, Lee RJ, Flaherty KT, McArthur GA. Improved survival with vemurafenib in melanoma with BRAF V600E mutation. N Engl J Med. 2011; 364:2507–2516. [PubMed: 21639808]
19. Hauschild A, Grob JJ, Demidov LV, Jouary T, Gutzmer R, Millward M, Rutkowski P, Blank CU, Miller WH Jr, Kaempgen E, Martin-Algarra S, Karaszewska B, Mauch C, Chiarion-Sileni V, Martin AM, Swann S, Haney P, Mirakhur B, Guckert ME, Goodman V, Chapman PB. Dabrafenib in BRAF-mutated metastatic melanoma: a multicentre, open-label, phase 3 randomised controlled trial. Lancet. 2012; 380:358–365. [PubMed: 22735384]

Author Manuscript Author Manuscript Author Manuscript Author Manuscript

20. Long GV, Trefzer U, Davies MA, Kefford RF, Ascierto PA, Chapman PB, Puzanov I, Hauschild A, Robert C, Algazi A, Mortier L, Tawbi H, Wilhelm T, Zimmer L, Switzky J, Swann S, Martin AM, Guckert M, Goodman V, Streit M, Kirkwood JM, Schadendorf D. Dabrafenib in patients with Val600Glu or Val600Lys BRAF-mutant melanoma metastatic to the brain (BREAK-MB): a multicentre, open-label, phase 2 trial. Lancet Oncol. 2012; 13:1087–1095. [PubMed: 23051966]
21. Villanueva J, Vultur A, Herlyn M. Resistance to BRAF inhibitors: unraveling mechanisms and future treatment options. Cancer Res. 2011; 71:7137–7140. [PubMed: 22131348]
22. Sullivan RJ, Flaherty KT. Resistance to BRAF-targeted therapy in melanoma. Eur J Cancer. 2013; 49:1297–1304. [PubMed: 23290787]
23. Kwekkeboom DJ, Kam BL, van Essen M, Teunissen JJ, van Eijck CH, Valkema R, de Jong M, de Herder WW, Krenning EP. Somatostatin-receptor-based imaging and therapy of gastroenteropancreatic neuroendocrine tumors. Endocr -Relat Cancer. 2010; 17:R53–R73. [PubMed: 19995807]
24. Van Essen M, Krenning EP, De Jong M, Valkema R, Kwekkeboom DJ. Peptide Receptor Radionuclide Therapy with radiolabelled somatostatin analogues in patients with somatostatin receptor positive tumours. Acta Oncol. 2007; 46:723–734. [PubMed: 17653893]
25. Forrer F, Uusijarvi H, Storch D, Maecke HR, Mueller-Brand J. Treatment with 177Lu-DOTATOC of patients with relapse of neuroendocrine tumors after treatment with 90Y-DOTATOC. J Nucl Med. 2005; 46:1310–1316. [PubMed: 16085587]
26. Miyake K, Hasunuma Y, Yagita H, Kimoto M. Requirement for VLA-4 and VLA-5 integrins in lymphoma cells binding to and migration beneath stromal cells in culture. J Cell Biol. 1992; 119:653–662. [PubMed: 1400595]
27. Juneja HS, Schmalsteig FC, Lee S, Chen J. Vascular cell adhesion molecule-1 and VLA-4 are obligatory adhesion proteins in the heterotypic adherence between human leukemia/lymphoma cells and marrow stromal cells. Exp Hematol. 1993; 21:444–450. [PubMed: 7680000]
28. Holzmann B, Gosslar U, Bittner M. alpha 4 integrins and tumor metastasis. Curr Top Microbiol Immunol. 1998; 231:125–141. [PubMed: 9479864]
29. Peng L, Liu R, Marik J, Wang X, Takada Y, Lam KS. Combinatorial chemistry identifies high-affinity peptidomimetics against $\alpha 4\beta 1$ integrin for in vivo tumor imaging. Nat Chem Biol. 2006; 2:381–389. [PubMed: 16767086]
30. Beaino W, Anderson CJ. PET Imaging of Very Late Antigen-4 in Melanoma: Comparison of 68Ga- and 64Cu-Labeled NODAGA and CB-TE1A1P-LLP2A Conjugates. J Nucl Med. 2014; 55:1856–1863. [PubMed: 25256059]
31. Wadas TJ, Eiblmaier M, Zheleznyak A, Sherman CD, Ferdani R, Liang K, Achilefu S, Anderson CJ. Preparation and biological evaluation of 64Cu-CB-TE2A-sst2-ANT, a somatostatin antagonist for PET imaging of somatostatin receptor-positive tumors. J Nucl Med. 2008; 49:1819–1827. [PubMed: 18927338]
32. Gourni E, Demmer O, Schottelius M, D'Alessandria C, Schulz S, Dijkgraaf I, Schumacher U, Schwaiger M, Kessler H, Wester HJ. PET of CXCR4 expression by a (68)Ga-labeled highly specific targeted contrast agent. J Nucl Med. 2011; 52:1803–1810. [PubMed: 22045709]
33. Reubi JC, Schar JC, Waser B, Wenger S, Heppeler A, Schmitt JS, Macke HR. Affinity profiles for human somatostatin receptor subtypes SST1–SST5 of somatostatin radiotracers selected for scintigraphic and radiotherapeutic use. Eur J Nucl Med. 2000; 27:273–282. [PubMed: 10774879]
34. Corneillie TM, Fisher AJ, Meares CF. Crystal structures of two complexes of the rare-earth-DOTA-binding antibody 2D12.5: ligand generality from a chiral system. J Am Chem Soc. 2003; 125:15039–15048. [PubMed: 14653738]
35. Kulkarni HR, Prasad V, Schuchardt C, Baum RP. Is there a correlation between peptide receptor radionuclide therapy-associated hematological toxicity and spleen dose? Recent Results Cancer Res. 2013; 194:561–566. [PubMed: 22918783]
36. Schadendorf D, Gawlik C, Haney U, Ostmeier H, Suter L, Czarnetzki BM. Tumour progression and metastatic behaviour in vivo correlates with integrin expression on melanocytic tumours. J Pathol. 1993; 170:429–434. [PubMed: 8105045]
37. Hart IR, Birch M, Marshall JF. Cell adhesion receptor expression during melanoma progression and metastasis. Cancer Metastasis Rev. 1991; 10:115–128. [PubMed: 1873852]

Author Manuscript Author Manuscript Author Manuscript Author Manuscript

38. Moretti S, Martini L, Berti E, Pinzi C, Giannotti B. Adhesion molecule profile and malignancy of melanocytic lesions. Melanoma Res. 1993; 3:235–239. [PubMed: 8219755]

39. Fani M, Del Pozzo L, Abiraj K, Mansi R, Tamma ML, Cescato R, Waser B, Weber WA, Reubi JC, Maecke HR. PET of somatostatin receptor-positive tumors using 64Cu- and 68Ga-somatostatin antagonists: the chelate makes the difference. J Nucl Med. 2011; 52:1110–1118. [PubMed: 21680701]

40. Nedrow JR, White AG, Modi J, Nguyen K, Chang AJ, Anderson CJ. Positron emission tomographic imaging of copper 64-and gallium 68-labeled chelator conjugates of the somatostatin agonist tyr3-octreotate. Mol Imaging. 2014; 13doi: 10.2310/7290.2014.00020

41. Quinn T, Zhang X, Miao Y. Targeted melanoma imaging and therapy with radiolabeled alpha-melanocyte stimulating hormone peptide analogues. G Ital Dermatol Venereol. 2010; 145:245–258. [PubMed: 20467398]

42. Siegrist W, Solca F, Stutz S, Giuffre L, Carrel S, Girard J, Eberle AN. Characterization of receptors for alpha-melanocyte-stimulating hormone on human melanoma cells. Cancer Res. 1989; 49:6352–6358. [PubMed: 2804981]

43. Miao Y, Whitener D, Feng W, Owen NK, Chen J, Quinn TP. Evaluation of the human melanoma targeting properties of radiolabeled alpha-melanocyte stimulating hormone peptide analogues. Bioconjugate Chem. 2003; 14:1177–1184.

44. Rosenkranz AA, Slastnikova TA, Durymanov MO, Sobolev AS. Malignant melanoma and melanocortin 1 receptor. Biochemistry (Mosc). 2013; 78:1228–1237. [PubMed: 24460937]

Author Manuscript Author Manuscript Author Manuscript Author Manuscript

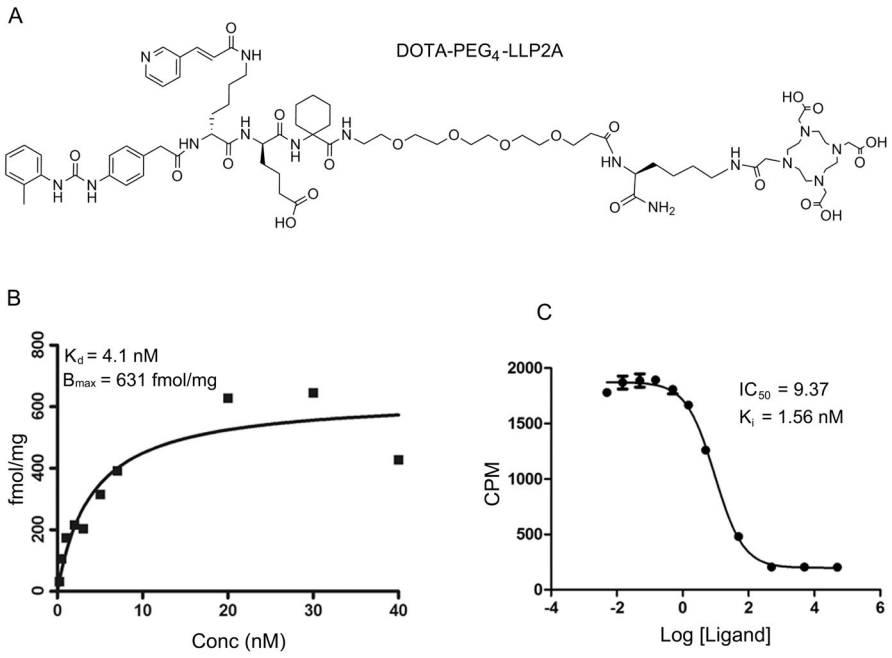

Figure 1.

Structure of DOTA-PEG_4-LLP2A (A). The binding of ^{177}Lu-DOTA-PEG_4-LLP2A to integrin $\alpha_4\beta_1$ was determined by saturation binding assay in B16F10 melanoma cells ($n = 3$ for each data point); The K_d is 4.1 ± 1.5 nM and the receptor concentration (B_{max}) is 631 ± 70.2 fmol/mg (B). The binding of Ga-DOTA-PEG_4-LLP2A to integrin $\alpha_4\beta_1$ was determined by competitive binding assay with ^{64}Cu-NODAGA-PEG_4-LLP2A (competitor) in B16F10 melanoma cells ($n = 4$ for each data point); the half maximal inhibitory concentration (IC_{50}) is 9.37 nM (95% confidence intervals 7.8–11.2), and the absolute inhibition constant (K_i) is 1.56 nM (95% confidence intervals 1.3–1.8) (C).

Author Manuscript Author Manuscript Author Manuscript Author Manuscript

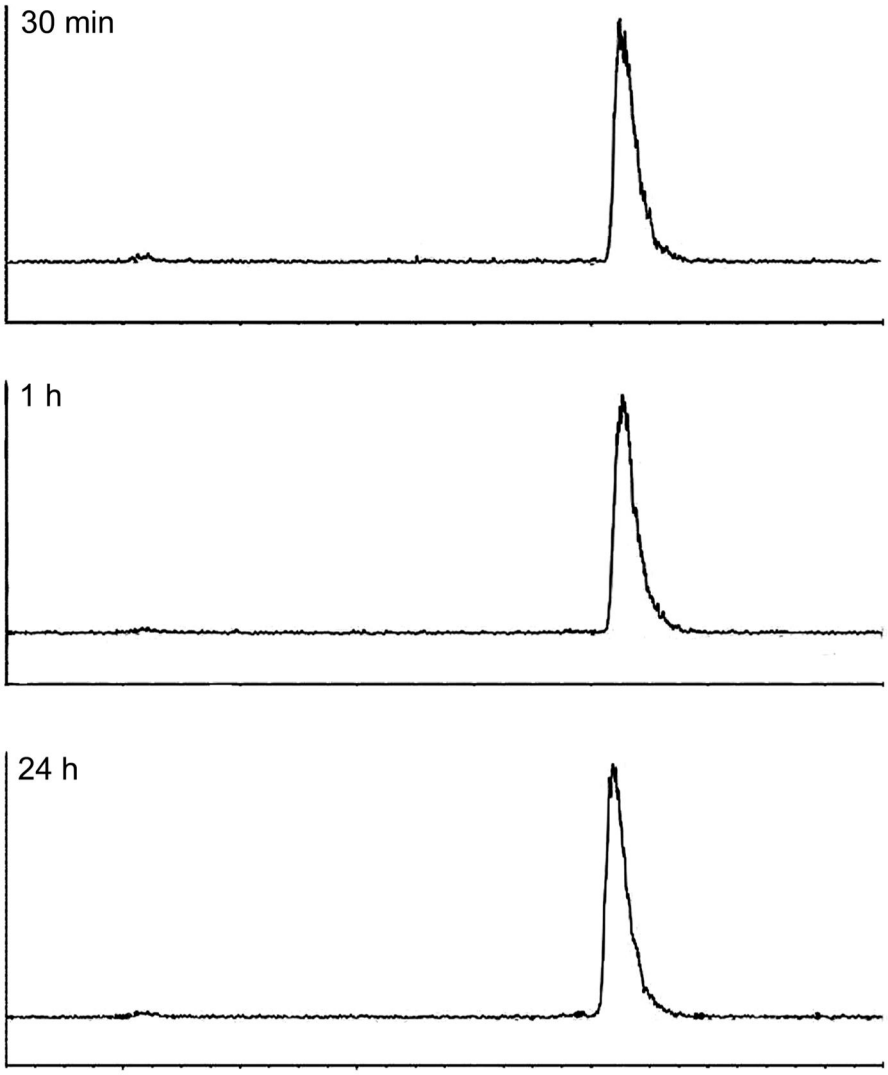

Figure 2.
Bench stability of ^{177}Lu-DOTA-PEG$_4$-LLP2A at 30 min, 1 and 24 h postlabeling.

Author Manuscript Author Manuscript Author Manuscript Author Manuscript

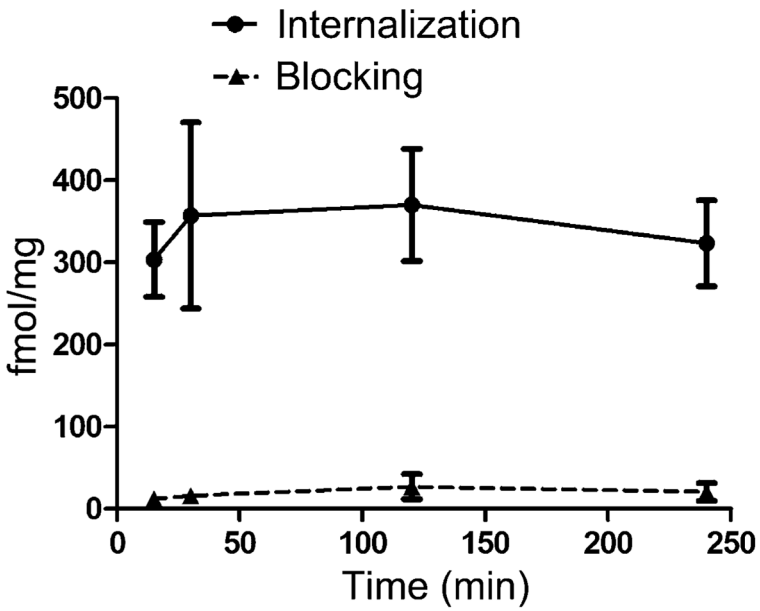

Figure 3.
Internalization of ^{177}Lu-DOTA-PEG$_4$-LLP2A (12 ng/well each) in B16F10 cells at 15, 30 min, 2 and 4 h (n = 3).

Author Manuscript Author Manuscript Author Manuscript Author Manuscript

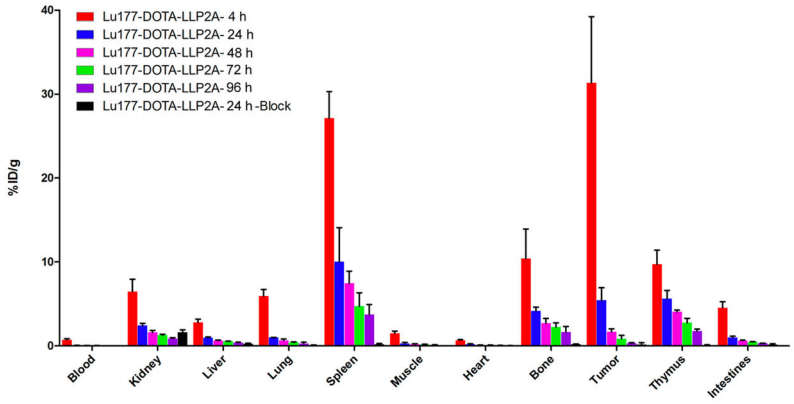

Figure 4.

Biodistribution of ^{177}Lu-DOTA-PEG$_4$-LLP2A (3.6 MBq, 90 ng) in B16F10 tumor-bearing mice at 4, 24, 48, 72, and 96 h postinjection, with or without excess LLP2A-PEG$_4$ as a blocking agent (n = 5).

Author Manuscript Author Manuscript Author Manuscript Author Manuscript

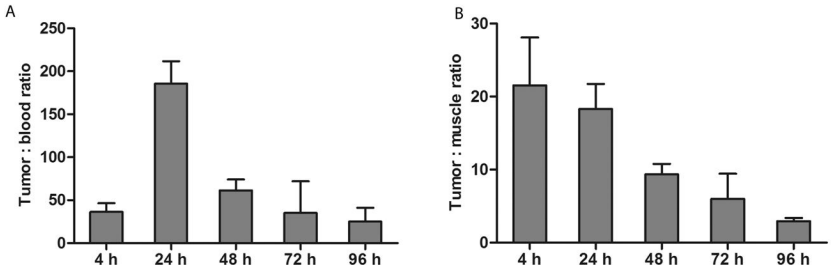

Figure 5.
Tumor/blood ratio (A) and tumor/muscle ratio (B) of ^{177}Lu-DOTA-PEG$_4$-LLP2A.

Author Manuscript Author Manuscript Author Manuscript Author Manuscript

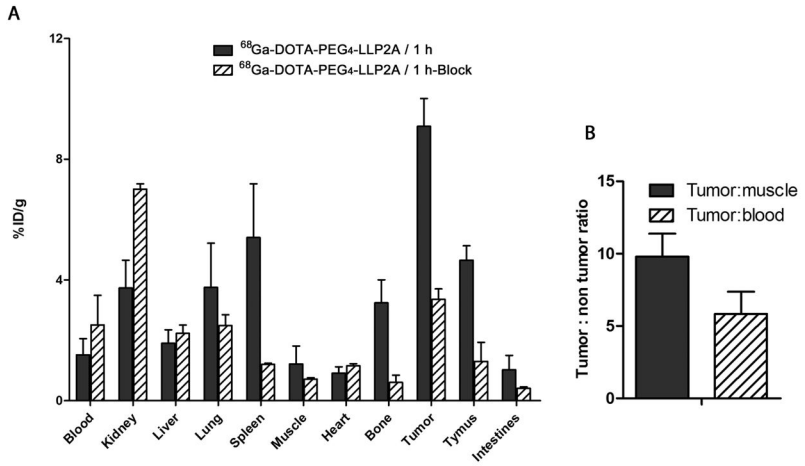

Figure 6.

Biodistribution of ^{68}Ga-DOTA-PEG$_4$-LLP2A (5.55 MBq, 277 ng) in B16F10 tumor-bearing mice at 1 h postinjection, with or without excess LLP2A-PEG$_4$ as a blocking agent (n = 4) (A). Tumor/blood and tumor/muscle ratio of ^{68}Ga-DOTA-PEG$_4$-LLP2A (B).

Author Manuscript Author Manuscript Author Manuscript Author Manuscript

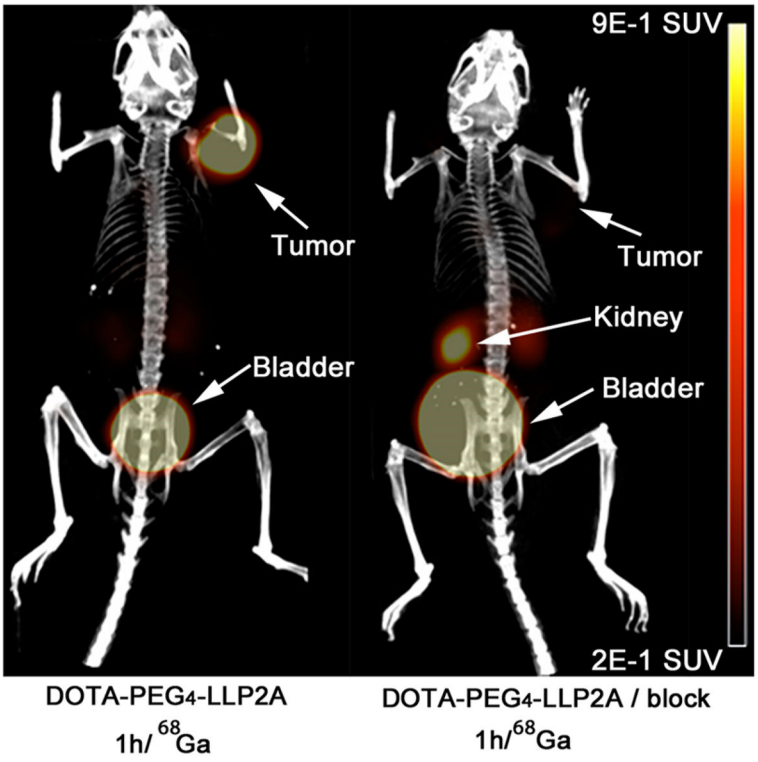

Figure 7.

Small-animal PET/CT images of ^{68}Ga-DOTA-PEG$_4$-LLP2A (7.4 MBq, 370 ng) in B16F10 tumor-bearing mice at 1 h postinjection, with or without excess LLP2A-PEG$_4$ as a blocking agent.

Author Manuscript Author Manuscript Author Manuscript Author Manuscript

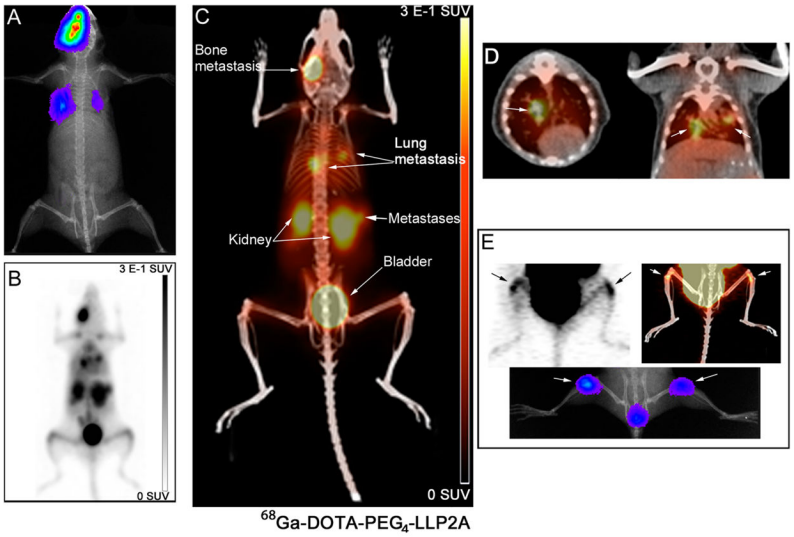

Figure 8.

Small animal PET/CT images of ^{68}Ga-DOTA-PEG$_4$-LLP2A in B16F10_Luc_tdT metastases at 1 h postinjection (6.5 MBq). Bioluminescence images show the site of metastases (lungs and bone) (A). PET maximum intensity projection (MIP) (B) and PET/CT MIP (C) show the uptake of the probe in the sites of metastasis. Horizontal and coronal sections of PET/CT fused images show uptake of the probe in the lung metastases (white arrows) (D). Horizontal sections of PET/CT image showing uptake of the probe in the bone metastases (white arrow) (E).